Available online at www.CivileJournal.org

Civil Engineering Journal

(E-ISSN: 2476-3055; ISSN: 2676-6957)

Vol. 10, No. 03, March, 2024

Experimental Study on Hollow Steel Sections Under Elevated Temperature

Prakash Murugan [1], Alireza Bahrami [2*], Vishal Murugan [1], Ajish Kumaran [1]

[1] *Department of Civil Engineering, College of Engineering and Technology, SRM Institute of Science and Technology, SRM Nagar, Kattankulathur – 603 203, Tamil Nadu, India.*

[2] *Department of Building Engineering, Energy Systems and Sustainability Science, Faculty of Engineering and Sustainable Development, University of Gävle, 801 76 Gävle, Sweden.*

Received 25 August 2023; Revised 07 February 2024; Accepted 12 February 2024; Published 01 March 2024

Abstract

Structures known as modular buildings are made in factories and then moved to construction sites, where they are assembled. The efficacy of modular structures under many uncertainties has to be thoroughly investigated as demand rises; fire is one such uncertainty. The purpose of this study is to ascertain how high temperature affects the components of modular constructions. In the current study, hollow steel columns and beams were taken into account as components of a modular construction. Using ABAQUS, several situations were examined depending on the span length to determine the important locations of the members. Experimental research was conducted on the critical regions identified by the analysis, and the results were contrasted with those of the analysis. A high-temperature localized heating furnace was used for the experimental testing. The findings demonstrated that for spans of 250 mm and 500 mm, the central area of the beams was essential, and the load-carrying capacity was six times less than that of heating at the extremities of the beams. Similar to the beams, columns exhibited less fluctuation than the beams and were weaker in the bottom area when exposed to high temperature. When compared to other places, the capacity was reduced by 1.1 times, and in Case 1, the capacity reduction with regard to loading was 1.68 times greater.

Keywords: Modular Building; Elevated Temperature; Hollow Steel Section; Critical Fire Region; Finite Element Analysis.

1. Introduction

Buildings undergo many natural and man-made disasters during their lifetime. One such type that has been given attention is the effect of seismicity. Many analytical and experimental research works have been conducted in this area. However, facts tell us that the number of people who lose their lives is not due to the direct effect of the earthquake but to indirect effects such as fire, among many other things [1]. Hence, it is crucial that the materials used in building construction can withstand a fire for a certain period of time. In this regard, it is important to keep in mind that at the temperatures that may be anticipated under fire conditions, the strength and deformation capabilities of regularly utilized building materials dramatically deteriorate [2]. The kind and quantity of combustible elements present affect this temperature development, among other factors. The term "fire resistance" refers to how long a building component can tolerate the heat exposure in accordance with the standard fire curve [3, 4]. The right performance criteria must be established before it is possible to assess a building component's fire resistance [5]. There are essentially two approaches that can be employed to determine fire resistance: an experimental approach and an analytical or fire engineering technique.

* Corresponding author: alireza.bahrami@hig.se

http://dx.doi.org/10.28991/CEJ-2024-010-03-014

The modular building technique is a rapidly expanding methodology that may be used instead of conventional on-site construction. A modular structure comprises several premade sections known as "modules" [6]. Modules are manufactured in a faraway place to create permanent residential or commercial structures and fabricated on-site. Apartments, schools, offices, and any other facility in which repeated units are desirable are all examples of modular construction [7]. Modular construction is utilized mainly for low-rise dwellings in America, Japan, and some areas of Europe. At the same time, the growing urban population necessitates the construction of additional high-rise structures [8].

Cast-in-place and prefabrication technologies were compared together with two common housing projects by Cao et al. [9]. Several methods, including on-site measurements and interviews, were used to acquire the data. The research was divided into several areas, including resource depletion, energy use, and construction waste discharge. The building health effect assessment system and the construction environmental performance evaluation system were utilized to compute the two construction technologies. With a total consumption drop of 20.49%, the outcome indicated that prefabricated houses were more energy efficient than traditional residential construction. Simplicity, homogeneity, repetition, and economies of scale are ideal design practices for high-rise structures. This building method's appeal stems from its inherent benefits over traditional construction methods. Excellent productivity, good quality, shorter timelines, less waste creation, efficiency of cost, and less generation of noise are just a few benefits.

A thorough conceptual framework was offered by Gunawardena et al. [10], which may be used to choose the ideal structural system depending on the circumstances. In order to optimize the building, a multidisciplinary approach will assess the structural systems, construction materials, constructability, cost of construction, and speed. They have discussed many optimization algorithm types that are employed in building design, how they may be modified to assess a prefabricated structure, and which elements would prevail as crucial performance indicators in the search for the best prefabricated modular building solution. Using a dynamic case study-based assessment, Boafo et al. [11] characterized prefabricated levels and analyze the performance of prefabricated modules while considering acoustic constraints, resistance to seismic forces, thermal properties, energy demand, and life cycle analysis of current prefabricated examples. The modules can be categorized into two groups based on the method of load transfer: self-supporting load-bearing modules and frame-supported modules [12]. The loads are distributed through the walls of the modules. Because of this point, the building heights are normally restricted to four to eight stories, and the compressive resistance of the walls is essential. On the other hand, for frame-supported modules, loads are distributed by edge beams attached to corner posts, and the posts need to have high compression resistance. Figure 1 shows a typical steel frame module.

Figure 1. Steel frame module

Modules are made to be lifted, and each module has specific lift points. Forklifts may be utilized in the manufacturer's yard, although cranes are typically employed to lift them [13]. Deflection parameters selected to safeguard delicate components are frequently used to define the quantity and placement of lift points. Existing standards, such as American Standard and DNV Offshore Standard, provide general guidance on the design of lifters. Developing countries need high-rise buildings for accommodation. Only the application of contemporary construction techniques built on standardization, unification, and typification can justify it economically.

The focus of experts' efforts is finding ways to lower construction costs. It should be highlighted that one of the most advanced and promising current trends in architectural and construction development worldwide is the use of off-site manufactured modules, or modular construction. Modular buildings are more durable than traditional buildings because of the independent engineering done in a factory [14]. The seismic performance of a frame structure was measured utilizing energy dissipation characteristics taking into consideration the seismic forces, thermal properties, and energy demand, revealing that the frame was stable and ductile up to high drift levels; there was no significant stiffness degradation with cyclic loading, and the structure had good energy dissipation per cycle in every loading step, demonstrating a higher seismic capacity for modular buildings [15]. Wu et al. [16] investigated how the mechanical

characteristics of a modular prefabricated steel-concrete composite internal joint (MPCIJ) were affected by the key parameters. MPCIJ was subjected to cyclic stress using the finite element analysis (FEA) software ABAQUS. Comparisons were made between the experimental and FEA results' hysteresis curves and mechanisms of failure. Various parameters' effects on structural performance were examined once the dependability of the numerical model was confirmed. The shear mechanism and bearing capacity calculation techniques were provided based on test and FEA findings. Kumar et al. [17] compared the structural and mechanical performances of the low-alloy cold-formed steel sections at different temperatures for developing high-fire performance steel structures. Precast structural systems are more economical than steel structures, according to Kim et al. [18], but their slower construction speed prohibits them from being widely used. This is because installing lateral bracing beams during erection is challenging. By swiftly and easily joining column-beam sections to beam sections, a structural approach is offered for lateral bracing during construction.

The lean tool kaizen was suggested by Nahmens et al. [19] as a practical and effective methodology for sustainability that concentrated on enhancing the environmental and socioeconomic performances of modular building processes. Numerous case examples are provided in this study to display how lean has an influence on the sustainability of modular housing. Ramaji & Memari [20] discussed multi-story modular building methods. They mentioned the challenges faced by structural designers when attempting to eliminate horizontal load transfer, gravity, and load path discontinuity. In addition to applicable building code requirements, the approaches for the modular system and modeling needed for assessing the buildings are given. The challenges of developing and detailing different structural sections and systems were also assessed. Additionally, any special structural safety factors that must be taken into account during design and construction were listed. Blast-resistant portable buildings are generally 40 feet long, 10–15 feet wide, and approximately 10 feet tall, and are subjected to blast impulses. It was found that during the blast reaction, there were a lot of sliding and flipping and requirements of positive pressure, and the traditional loading standards were the criteria for an appropriate degree of significance and building protection. Fireproofing measures with three layers of gypsum boards can safeguard the columns and ensure a 3-hour fire-resistance rating. The fireproofing measure with a layer of gypsum board and mineral wool experienced early gypsum board failure and a smaller rating [21].

A recent study by academicians from the University of Cambridge and Edinburgh Napier University found that modular buildings were able to save almost 28000 metric tons of carbon (i.e., approximately 45% less carbon) compared to traditional methods, as illustrated in Figure 2 [22]. Embodied carbon, which is released during the production and transportation of materials, accounts for 11% of global emissions, which is more than that of the carbon produced by the aviation and shipping industries combined and can also be reduced.

Figure 2. Modular building in Cambridge center for housing and planning research

The significance of the research is that modular systems can be utilized in explosively hazardous areas, such as petroleum areas and chemical processing industries [23]. It will also help us determine the areas of failure and what can be done to reduce the failure of the modules. With increasing attention given to high-density urban areas and limited working spaces, modular prefabrication can act as an excellent replacement for conventional buildings [21].

However, previous research failed to identify the influence of elevated temperatures and identify the critical region in a hollow steel section. The critical region under high temperatures is the portion where heating the small part of the member gives a similar reaction to heating the entire member. A small-intensity fire in the critical region could trigger the global collapse of the structure. This article will also act as a research foundation for future temperature studies of modular elements. The aim of the current study is to determine the behavior of beams and columns of a modular system (sub-assemblage element) analytically and experimentally under elevated temperature to find the critical region. Observing the critical region under fire would help engineers strengthen the structural members to perform well under fire scenario. This article includes an analytical study of the elements of modular buildings, such as beams and columns, under different load cases at different locations, and the performance of the critical section is obtained using an experimental study.

2. Material and Methods

The methodology of this research is represented in Figure 3.

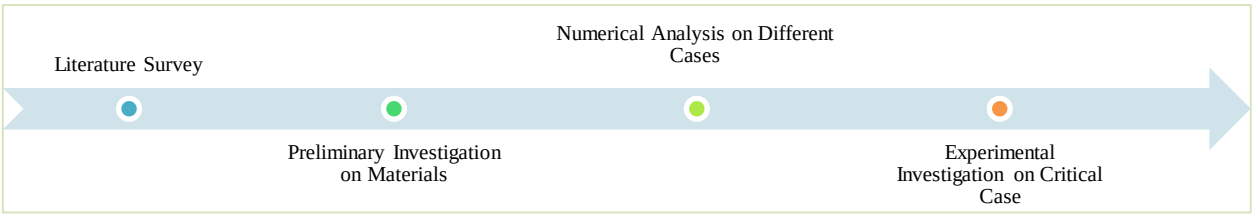

Figure 3. Methodology of current research work

2.1. Hot-Rolled Sections

Hot-rolled mild steel sections were taken for analysis and experimental purposes because it is simpler to produce, shape, and form hot-rolled steel [24]. Starting with a billet of still steel that has been heated to 1700 °F, the steel is rolled through the mill into the desired shape and is then cooled [25]. It has the properties of increased toughness and ductility and can be made into any shape. Hot-rolled steel angles or hollow sections are frequently used as corner posts. Moreover, the modular industry employs a variety of module shapes, including slope-end, stepped, faceted, and tapered modules [26]. The rectangular-shaped module, however, continues to be popular in buildings. Note that while corner-supported modules are unlikely to be utilized, wall-supported modules are compatible with any shape. Modular buildings are usually constructed in steel sections, and mostly either channel sections or hollow sections are used [27]. Due to their high strength, excellent ductility, light weight, and other advantages, square hollow steel tubular sections are frequently employed in the construction of steel [28, 29]. Steel has poor fire resistance, and hence, it is important to study fire in steels, as they form the primary component of modular buildings [30]. In this article, hollow sections are taken into consideration, as the number of studies on these sections is very low.

3. Analytical Study of Beams and Columns at Elevated Temperature

3.1. Analysis of Beams

The models were created, and the necessary studies were carried out using the FEA software ABAQUS. A total of 60 beams were modeled because of the variation in loading and temperature applications at different locations of the beams. Finite element models with a constant height of 1.5 m, outside dimensions of 100 mm × 100 mm, and a thickness of 5 mm were created to do the numerical analyses. The predefined temperature was set to 29 °C. To conduct the necessary FEA, thermal characteristics such as density, thermal conductivity, and specific heat were needed. A coupon test was performed, and the corresponding results are listed in Table 1. Table 2 presents these temperature-dependent variations in value along with the respective temperatures.

Table 1. Coupon test results

Specimen No.	Average thickness (mm)	Yield stress (N/mm^2)	Ultimate stress (N/mm^2)	Percentage of elongation
1	4.8	300.06	480.86	23.33
2	4.7	317.72	491.88	21.67

Table 2. Properties of hollow steel section for finite element modeling [31]

Temperature (°C)	Young's modulus (N/mm^2)	Thermal conductivity (W/m K)	Linear expansion	Specific heat (J/kg K)
29	200000	53.33	0	439.8
100	200000	50.67	0.00001248	487.6
200	180000	47.34	0.00001288	529.8
300	160000	44.01	0.00001328	564.7
400	140000	40.68	0.00001368	605.9
500	120000	37.35	0.00001408	666.5
600	62000	34.02	0.00001448	759.9
700	26000	30.69	0.00001488	1008.2
800	18000	27.3	0.0000141	803.3

Other properties include a Poisson ratio of 0.3 and a steel density of 7850 kg/m^3. To obtain the plasticity values, a coupon test was done for the steel material [32].

The type of analysis performed was transient because of the involvement of the temperature and time. Analysis was performed on various segments, such as 250 mm, 500 mm, 750 mm, and 1500 mm, under different loading cases, including 10%, 20%, 30%, 40%, and 50%. A temperature of 800 °C was taken since the hot-rolled sections are subjected to rolling at temperatures varying from 850–1200 °C so that the critical temperature can be achieved. Figure 4 depicts the cases taken for the application of the temperature to various regions of the beams.

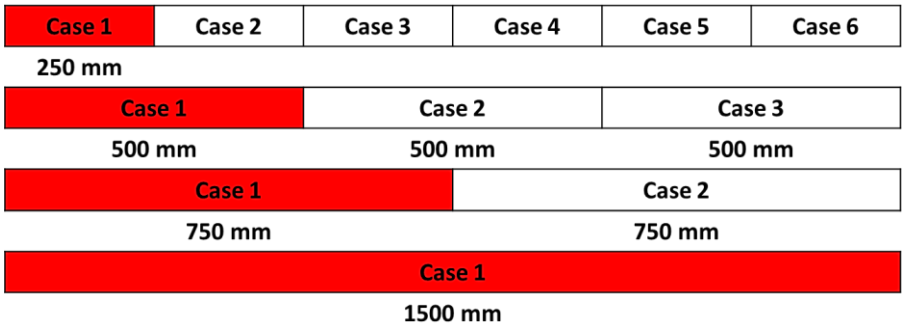

Figure 4. Different cases taken for analysis of beams

3.2. Analysis of Columns

A total of 60 columns were modeled owing to the variation in loading and temperature applications at different locations of the columns. Finite element models with a constant height of 1.5 m with outside dimensions of 100 mm × 100 mm and a thickness of 5 mm were created to conduct the numerical analyses. The predefined temperature was set to 29 °C. Analysis was performed on various segments, such as 250 mm, 500 mm, 750 mm, and 1500 mm, under different loading cases, including 50%, 60%, 70%, 80%, and 90%, with the view that the column can take a large amount of load. A base plate with dimensions of 200 mm × 200 mm was given with a thickness of 20 mm to apply the load. Surface-to-surface connections were provided. The type of support given was pinned support, which was provided at the bottom of the column. Figure 5 shows the cases taken for the application of the temperature to various regions of the columns. Figure 6 indicates a typical model and mesh of the column.

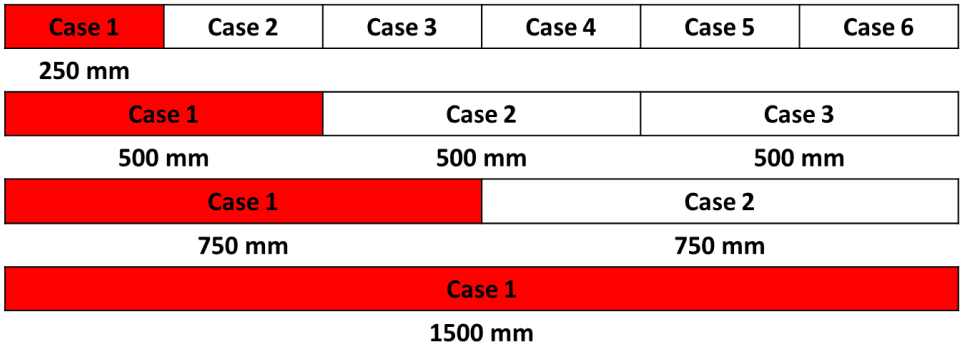

Figure 5. Different cases taken for analysis of columns

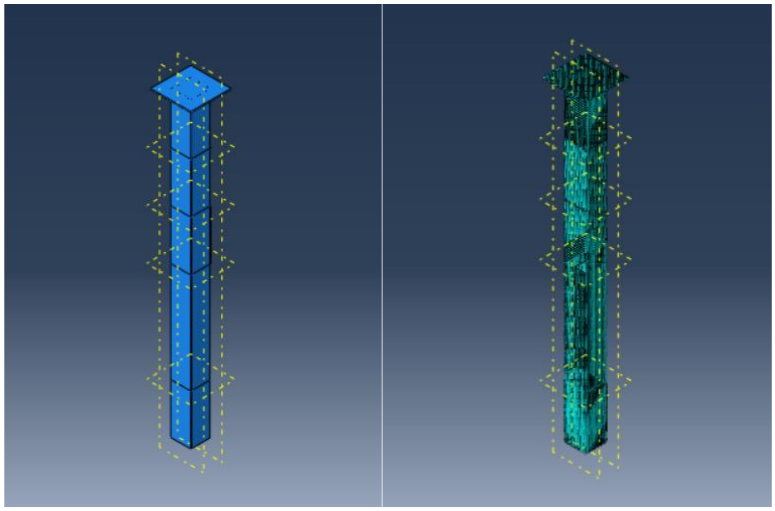

Figure 6. Typical model and mesh of column

4. Experimental Study of Beam and Column at Elevated Temperature

4.1. Testing Materials

Two specimens of hollow square steel sections were taken with dimensions of 100 mm × 100 mm × 5 mm, which were 1500 mm long, of which one was a beam, and another was taken as a column. The type of material used was hot-rolled steel [33]. The steel was painted, and then markings were placed on the beam and column. Figure 7 displays the specimens before and after painting.

Figure 7. Specimens before and after painting

4.2. Temperature Test on Beam

Beam was placed with a boundary condition of 100 mm from either side of the beam, and the type of loading given was four-point loading, and loading was given at l/3 distance from either side of the boundary conditions. The type of support provided was pinned support. Based on the analytical results, the middle section of the beam (i.e., the middle 500 mm of the beam) was found to be critical, and hence, the oven was placed at the center. A girder was prepared to apply the load with a gap in the middle so that the oven could be fitted in the place. An in-house fabricated localized heating furnace was utilized to apply the temperature. The oven could reach temperatures up to 1000 °C. It could fit a member of a cross section of 125 mm × 125 mm and a span of 600 mm. Loading was applied to the beam with the help of a manual-type loader using a hydraulic jack. A test load of 25 kN at a rate of 5 kN and the deflection of the beam were taken employing the two dial gauges located at the point of loading, which can be seen in Figures 8 and 9. The test load was given based on a certain percentage based on the ultimate load found through the analytical study. After the application of the test load, the loading was locked, and the temperature was set to 200 °C according to the result obtained from the analysis. The time taken to reach 200 °C was noted for a regular interval of one minute. Once the oven reached the temperature mentioned, the temperature was measured utilizing an infrared gun at the midpoints marked at 100 mm intervals from the center of the beam (a total of 9 points were marked on the beam) at regular intervals, and the deflection at both dial gauges was noted regularly at intervals of 10 minutes. After 4 hours, the furnace was switched off, cooling was performed for 90 minutes, and the deflection and temperature values were again taken similarly at regular intervals for 10 minutes.

Figure 8. Experimental test setup for beam at elevated temperature

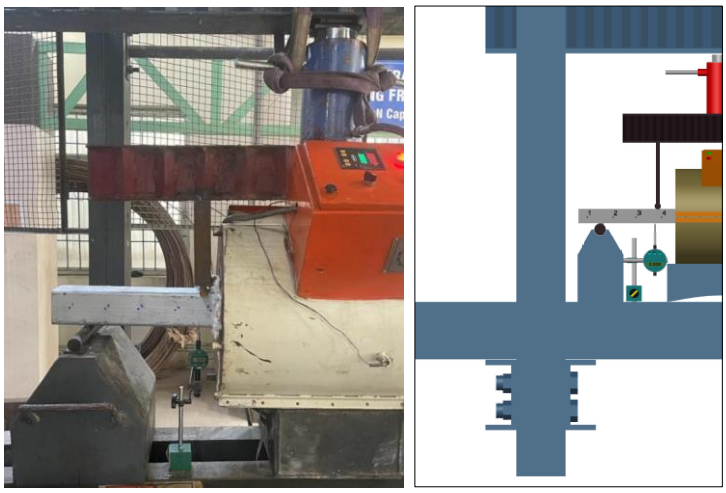

Figure 9. Dial gauge at point of loading

4.3. Temperature Test on Column

As the bottom of the columns was found to be critical, with the knowledge that usually the fire starts from the bottom of the column, the oven was placed 10 cm from the bottom of the column. Six points were marked on the column above at 10 cm to measure the temperature. Similarly, a point was marked 10 cm from the bottom of the column to take the readings. The test load of 250 kN was given initially, and then the temperature was provided. A dial gauge was placed to take the deflection values regularly, similar to those of the beam. Initially, it was provided up to a temperature of 600 °C, and then it was kept constant for 4 hours, and temperatures were taken from center points through infrared thermometers at regular intervals of 10 minutes. After that, the temperature input was stopped, cooling was done for 4 hours, and readings were taken similarly every 10 minutes. Figure 10 illustrates the experimental test setup for the column at the elevated temperature.

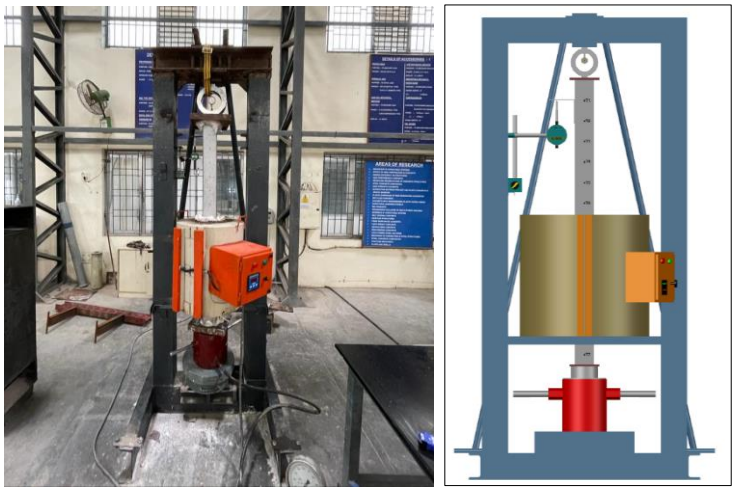

Figure 10. Experimental test setup for column at elevated temperature

5. Results and Discussion

5.1. Analytical Results of Beams

The time taken for the specimen to fail, the temperature the specimen was able to handle before failing, and the deflection values obtained during the time of failure taken from the analysis of the beams for different loadings at various locations were tabulated and compared to obtain the cooling behavior of the beams.

5.1.1. Effect of Temperature on 250 mm of Beams

The effect of the temperature on a region of 250 mm of the beams is demonstrated in Figure 11. A minimal effect can be observed as the temperature covers only 250 mm of the whole span. Case 3 with 50% loading was critical in terms of the temperature, and it was able to take 5 times less temperature when compared to 50% loading of Case 1. The time taken for Case 3 under 50% loading is 6.25 times less than that of Case 1 under 50% loading. From the analysis, it was found that the maximum deflection was found at 10% loading under Case 2. This must be because, with less loading, the effect of expansion on the beams with respect to the temperature might have been high. Table 3 summarizes the analytical results for 250 mm of the beams.

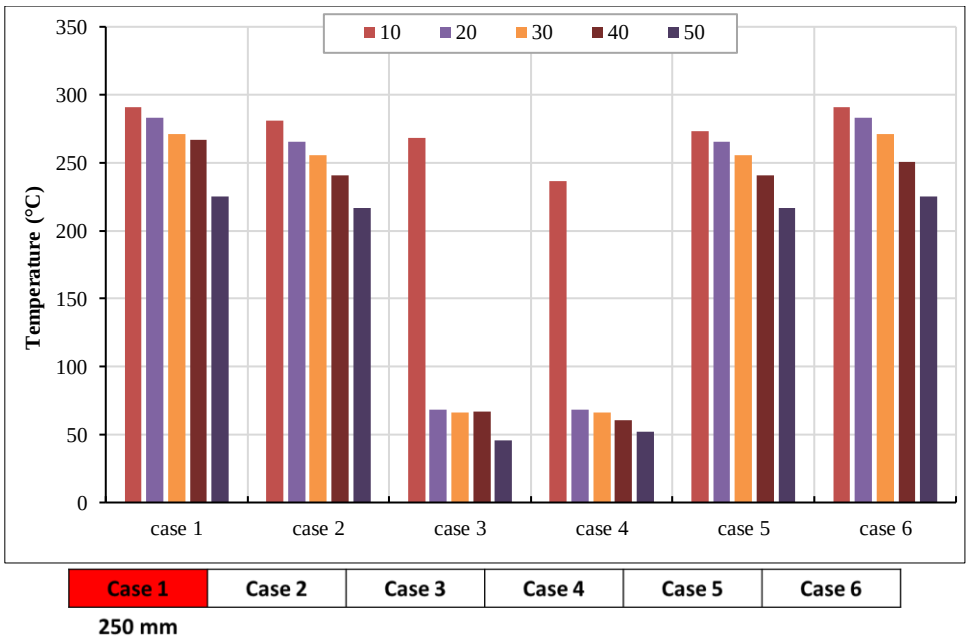

250 mm

(a)

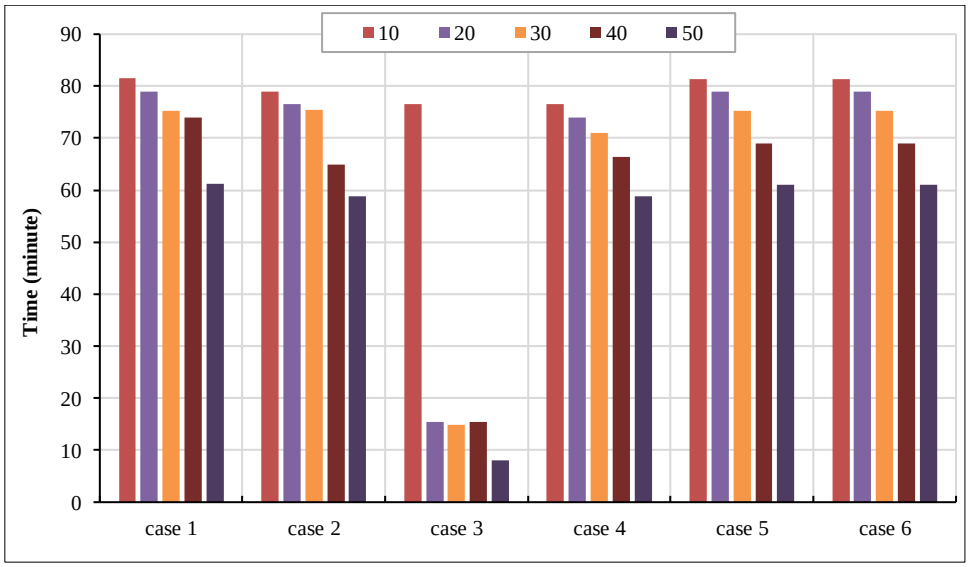

(b)

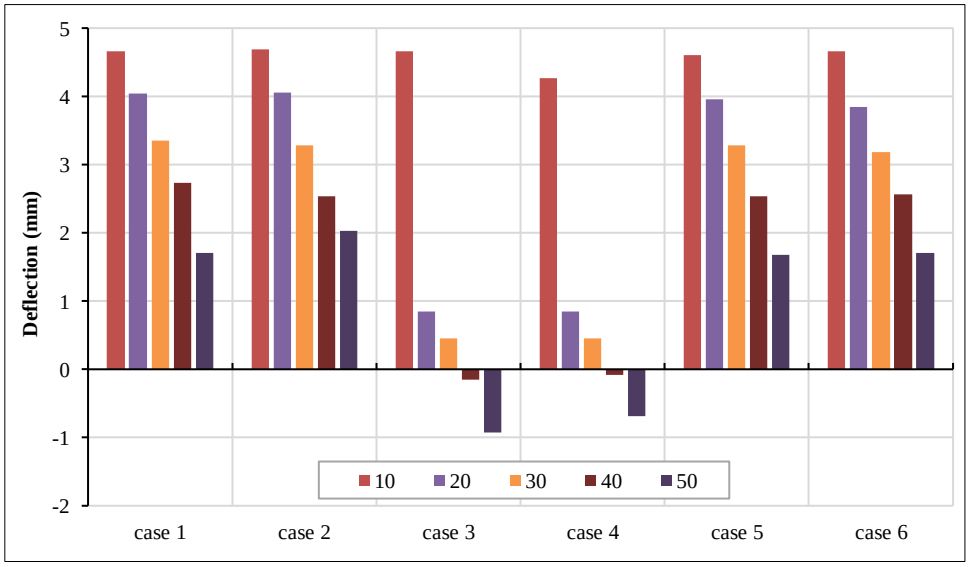

(c)

Figure 11. (a) Temperature for 250 mm of beams, (b) Time for 250 mm of beams, (c) Deflection for 250 mm of beams

Table 3. Analytical results for 250 mm of beams

Length	Type of cases	Load percentage (%)	Corresponding applied load (kN)	Temperature resisted (°C)	Time of resistance (minute)	Deflection (mm)
250 mm	Case 1	10	13.6	290.7	81.4	4.6
		20	27.2	282.7	79	4
		30	40.8	270.7	75.2	3.3
		40	54.4	266.5	73.9	2.7
		50	68	225	61.1	1.7
	Case 2	10	13.6	281	79	4.6
		20	27.2	265.3	76.5	4
		30	40.8	255.5	75.4	3.2
		40	54.4	240.8	64.8	2.2
		50	68	216.6	58.8	2
	Case 3	10	13.6	268	76.5	4.6
		20	27.2	68	15.5	0.8
		30	40.8	66	14.9	0.4
		40	54.4	64.5	14.7	-0.1
		50	68	45.7	8	-0.9
	Case 4	10	13.6	236.6	76.5	4.2
		20	27.2	68	74	0.8
		30	40.8	66	70.9	0.4
		40	54.4	60.5	66.3	-0.08
		50	68	52	58.8	-0.7
	Case 5	10	13.6	273.3	81.4	4.6
		20	27.2	265.3	79	3.9
		30	40.8	255.5	75.2	3.2
		40	54.4	240.8	68.9	2.5
		50	68	216.6	61.1	1.6
	Case 6	10	13.6	290.7	81.4	4.6
		20	27.2	282.7	79	3.8
		30	40.8	270.7	75.2	3.1
		40	54.4	250.5	68.9	2.5
		50	68	225.3	61.1	1.7

5.1.2. Effect of Temperature on 500 mm of Beams

Figure 12 depicts the effect of the temperature on a region of 500 mm of the beams. The effect can be seen clearly as 1/3 of the span is getting heated. Case 2 with 50% loading was critical in terms of the temperature, and it was able to take 3.45 times less temperature when compared to 50% loading of Case 1. It can also be found that Case 1 and Case 3 had similar effects on the temperature of the beams. The time taken for Case 2 under 50% loading is 4.9 times less than that of Case 1 under 50% loading. The maximum deflection was found at 10% loading under Case 2. Table 4 provides the analytical results for 500 mm of the beams.

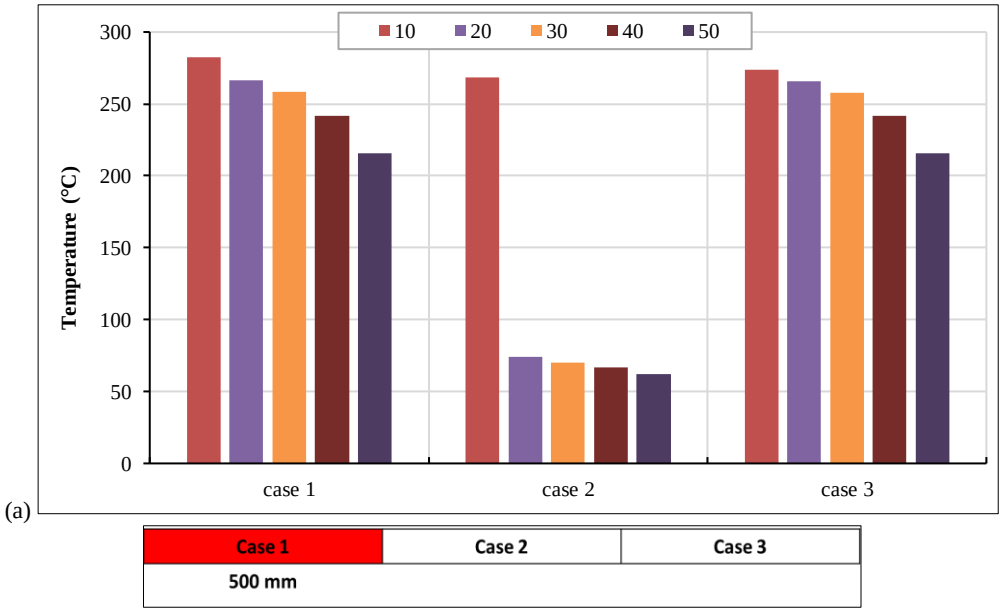

(a)

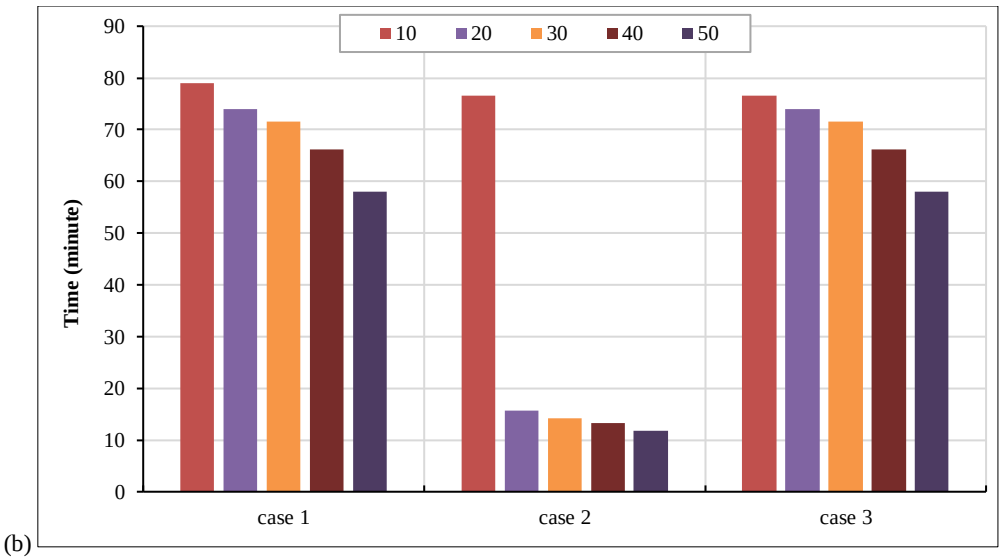

(b)

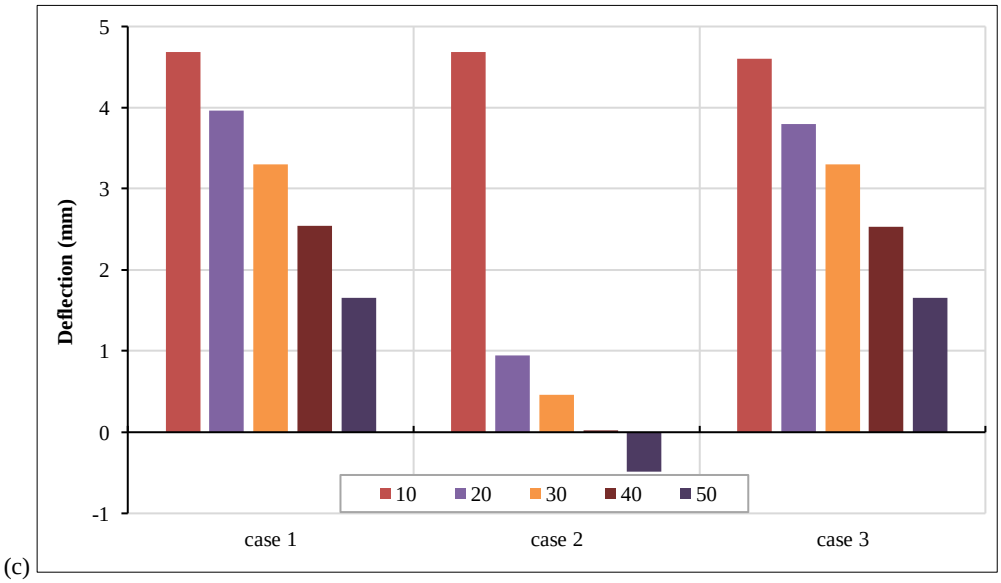

(c)

Figure 12. (a) Temperature for 500 mm of beams, (b) Time for 500 mm of beams, (c) Deflection for 500 mm of beams

Table 4. Analytical results for 500 mm of beams

Length	Type of cases	Load percentage (%)	Corresponding applied load (kN)	Temperature resisted (°C)	Time of resistance (minute)	Deflection (mm)
500 mm	Case 1	10	13.6	282.76	79	4.69
		20	27.2	266.7	74	3.962
		30	40.8	158.7	71.54	3.3
		40	54.4	241.5	66.16	2.53
		50	68	215.4	58.05	1.659
	Case 2	10	13.6	268.45	76.5	4.69
		20	27.2	74	15.76	0.947
		30	40.8	70.13	14.26	0.46
		40	54.4	67	13.3	0.019
		50	68	62	11.77	-0.49
	Case 3	10	13.6	274	76.5	4.6
		20	27.2	266	74	3.8
		30	40.8	258	71.53	3.3
		40	54.4	241.5	66.1	2.53
		50	68	215.4	58.05	1.659

5.1.3. Effect of Temperature on 750 mm of Beams

The effect of the temperature on a region of 750 mm of the beams is shown in Figure 13. The effect is obvious, as 1/2 of the span is subjected to high temperatures. Case 1 and Case 2 had similar kinds of responses in terms of the temperature resisted when half of the beams was subjected to heating. It was found that the maximum deflection was at 10% loading in Case 1 and Case 2, both indicating similar values. Table 5 displays the analytical results for 750 mm of the beams.

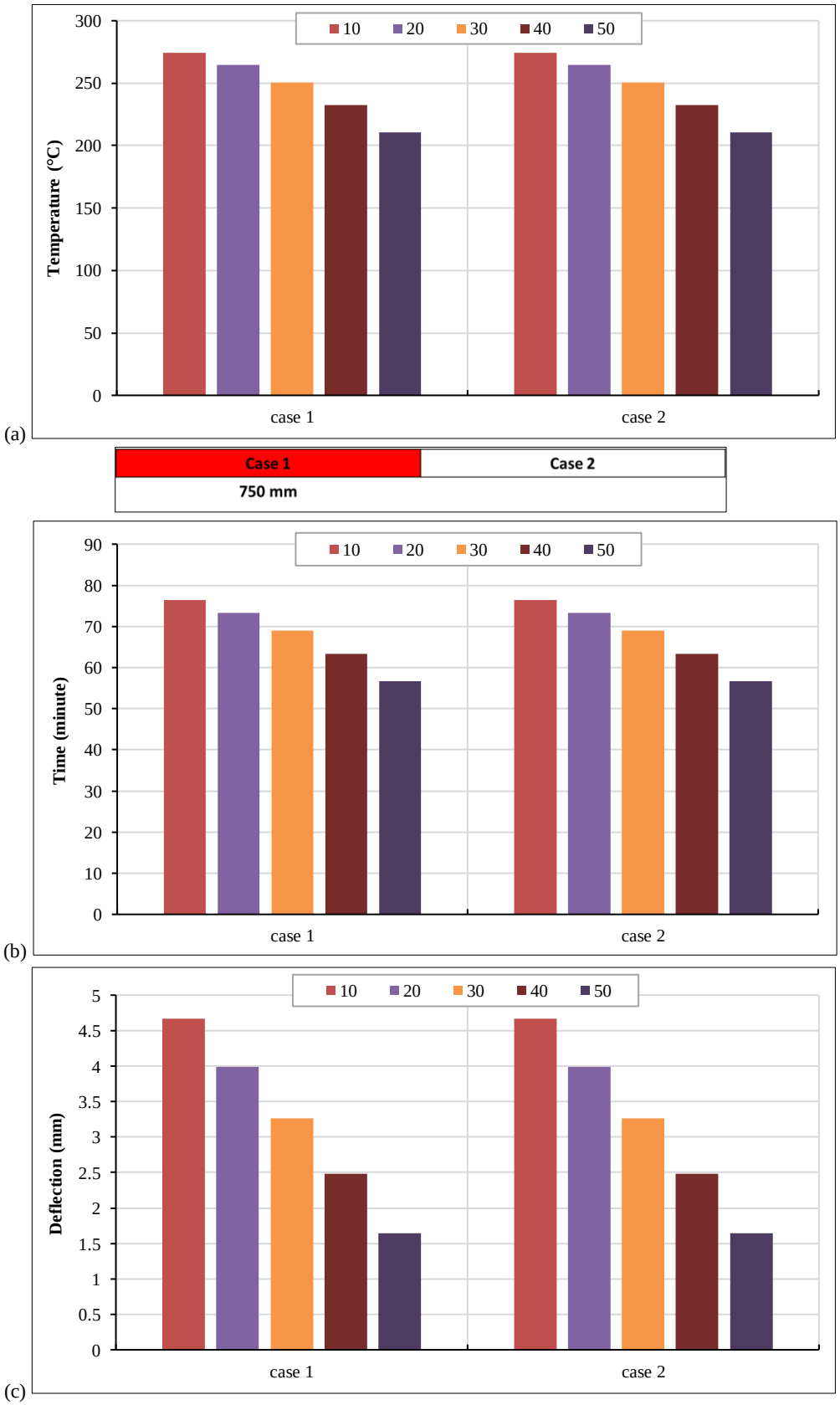

Figure 13. (a) Temperature for 750 mm of beams, (b) Time for 750 mm of beams, (c) Deflection for 750 mm of beams

Table 5. Analytical results for 750 mm of beams

Length	Type of cases	Load percentage (%)	Corresponding applied load (kN)	Temperature resisted (°C)	Time of resistance (minute)	Deflection (mm)
750 mm	Case 1	10	13.6	274	76.5	4.67
		20	27.2	264.6	73.36	3.99
		30	40.8	250.76	69	3.268
		40	54.4	232.5	63.36	2.48
		50	68	210.76	56.59	2.48
	Case 2	10	13.6	274	76.5	4.67
		20	27.2	264.6	73.36	3.99
		30	40.8	250.76	69	3.268
		40	54.4	232.5	63.36	2.48
		50	68	210.76	56.59	1.64

5.1.4. Effect of Temperature on 1500 mm of Beams

Figure 14 represents the effect of the temperature for a region of 1500 mm of the beams. The overall span is subjected to high temperature and becomes less effective (Table 6).

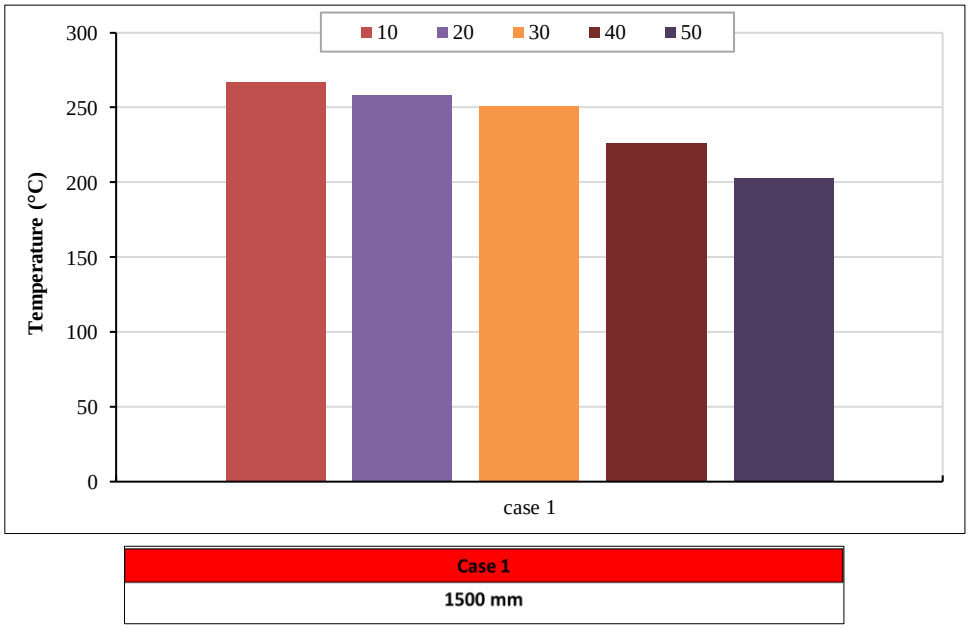

(a)

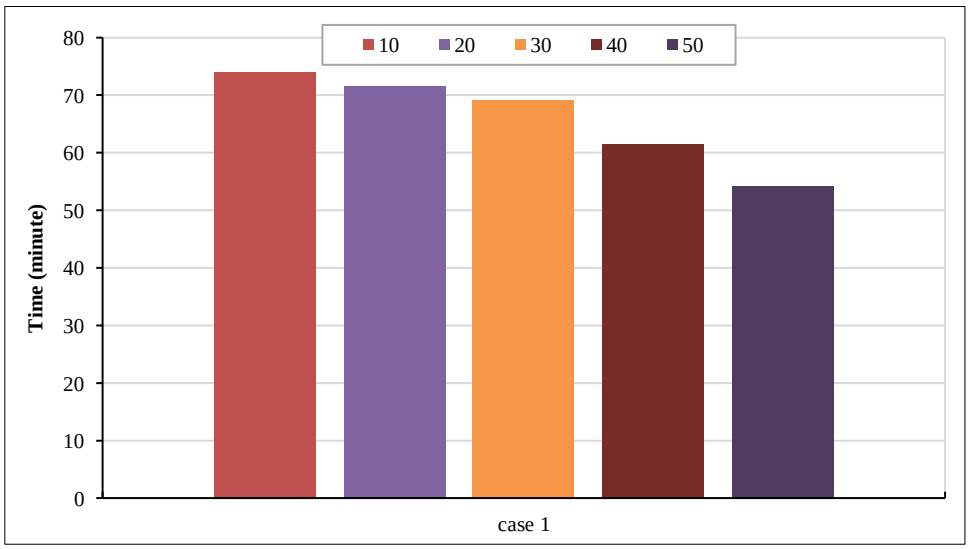

(b)

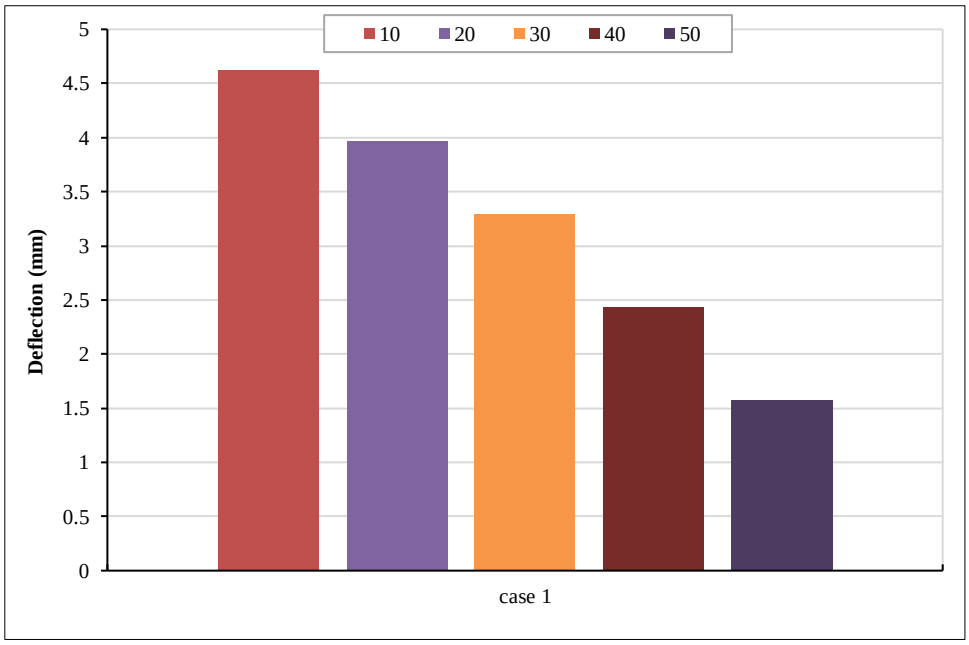

(c)

Figure 14. (a) Temperature for 1500 mm of beams, (b) Time for 1500 mm of beams, (c) Deflection for 1500 mm of beams

Table 6. Analytical results for 1500 mm of beams

Length	Type of cases	Load percentage (%)	Corresponding applied load (kN)	Temperature resisted (°C)	Time of resistance (minute)	Deflection (mm)
1500 mm	Case 1	10	13.6	266.7	74	4.62
		20	27.2	258.76	71.53	3.97
		30	40.8	250.76	69	3.3
		40	54.4	226.76	61.56	2.44
		50	68	202.76	54.1	1.58

Hence, it was finally concluded that the critical case of the beams was Case 2 in the 500 mm case and Cases 3 and 4 in the 250 mm case, demonstrating that the critical region was in the middle portion of the beams.

5.2. Analytical Results of Columns

The temperature, time, and deflection variations for the columns are presented in this section for different types of loadings at various locations. There were no significant changes with respect to the temperature at various locations, and the change was minimal. In addition, it was found that there was a symmetry in values on the ends of the columns.

5.2.1. Effect of Temperature on 250 mm of Columns

The effect of the temperature for a region of 250 mm of the columns is illustrated in Figure 15. Minimal effect can be observed as the temperature covers only 250 mm of the whole span. Table 7 displays the temperature at which the columns exceed the ultimate stress found using the coupon test. It can be seen from the table that Case 6 with 90% loading was critical in terms of the temperature, but the difference in the temperature was not as significant as in the columns. Case 3 was critical with 90% loading. The maximum deflection was witnessed in Case 5 with 90% loading.

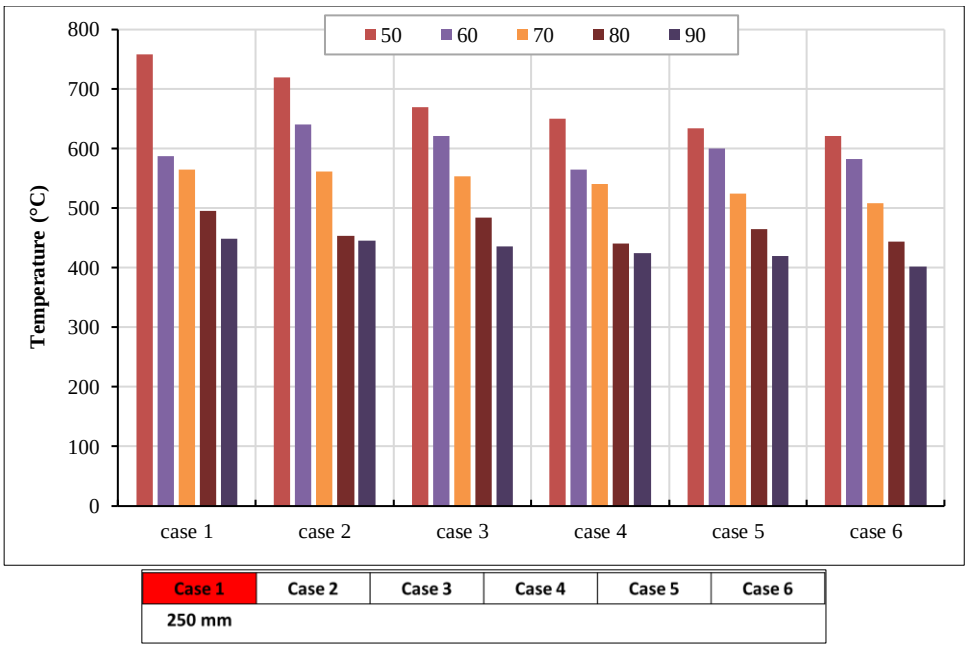

(a)

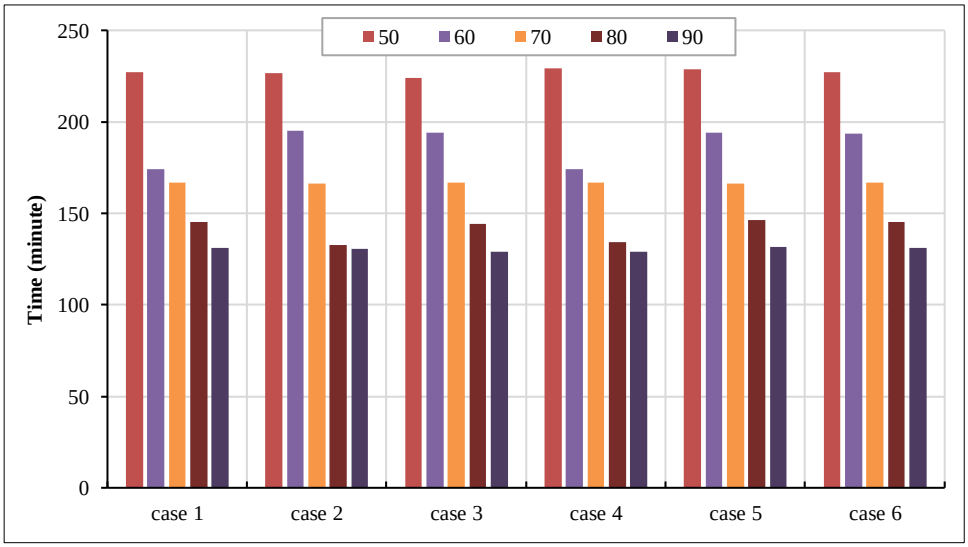

(b)

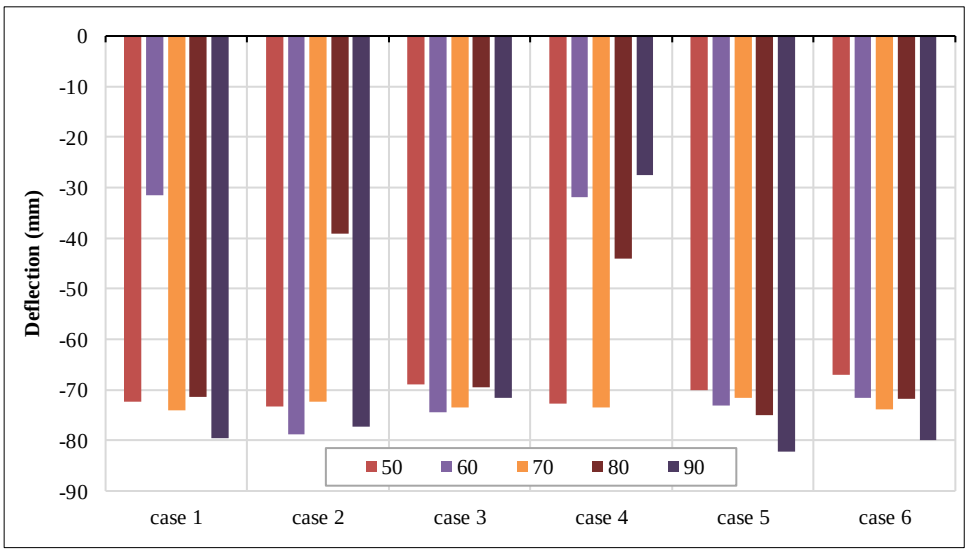

(c)

Figure 15. (a) Temperature for 250 mm of columns, (b) Time for 250 mm of columns, (c) Deflection for 250 mm of columns

Table 7. Analytical results for 250 mm of columns

Length	Type of cases	Load percentage (%)	Corresponding applied load (kN)	Temperature resisted (°C)	Time of resistance (minute)	Deflection (mm)
250 mm	Case 1	50	463.5	758	226.95	-72.25
		60	556.2	588	174.15	-31.5
		70	648.9	565	166.95	-74.09
		80	741.6	495.9	145.35	-71.45
		90	834.3	449.6	130.95	-79.6
	Case 2	50	463.5	720.4	226.38	-73.3
		60	556.2	641.1	195.35	-78.7
		70	648.9	561.1	166.48	-72.4
		80	741.6	453.7	132.8	-39.14
		90	834.3	446	130.4	-77.29
	Case 3	50	463.5	669.37	224.02	-68.9
		60	556.2	622.1	194.14	-74.5
		70	648.9	554.1	166.75	-73.4
		80	741.6	483.6	144.33	-69.5
		90	834.3	435.2	129	-71.5
	Case 4	50	463.5	650.8	229	-72.7
		60	556.2	564.8	174.2	-31.8
		70	648.9	541.5	166.6	-73.4
		80	741.6	440.8	134	-44.1
		90	834.3	425.4	129.05	-27.43
	Case 5	50	463.5	634.12	228.8	-70.14
		60	556.2	600	193.9	-73.07
		70	648.9	524.7	166.25	-71.67
		80	741.6	464.78	146.3	-75.08
		90	834.3	419.66	131.4	-82.3
	Case 6	50	463.5	621	226.95	-67.02
		60	556.2	581.9	193.35	-71.65
		70	648.9	508.2	166.95	-73.8
		80	741.6	444.8	145.35	-71.7
		90	834.3	401.9	130.95	-79.86

5.2.2. Effect of Temperature on 500 mm of Columns

The effect of the temperature for a region of 500 mm of the columns is depicted in Figure 16. Here, all the cases showed similar trends, but Case 1 with 90% loading indicated faster failure than the other cases. In accordance with the time variations of the columns subjected to heating, it was found that Case 1 and Case 3 displayed similar trends. Case 2 with 90% loading failed faster than the other cases. Case 1 with 90% loading exhibited higher deflection than the other cases. Table 8 demonstrates the analytical results for 500 mm of the columns.

(a)

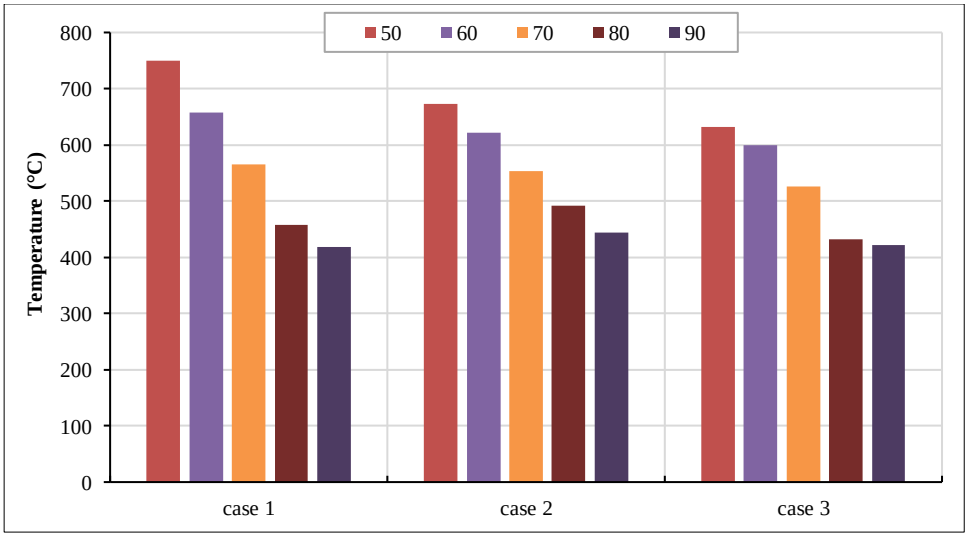

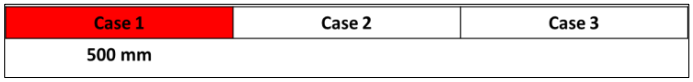

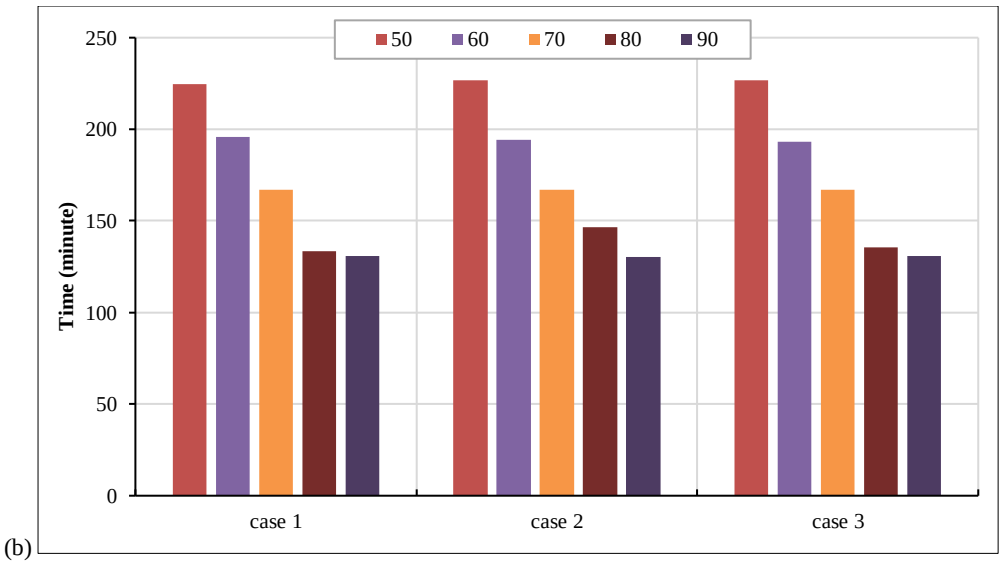

(b)

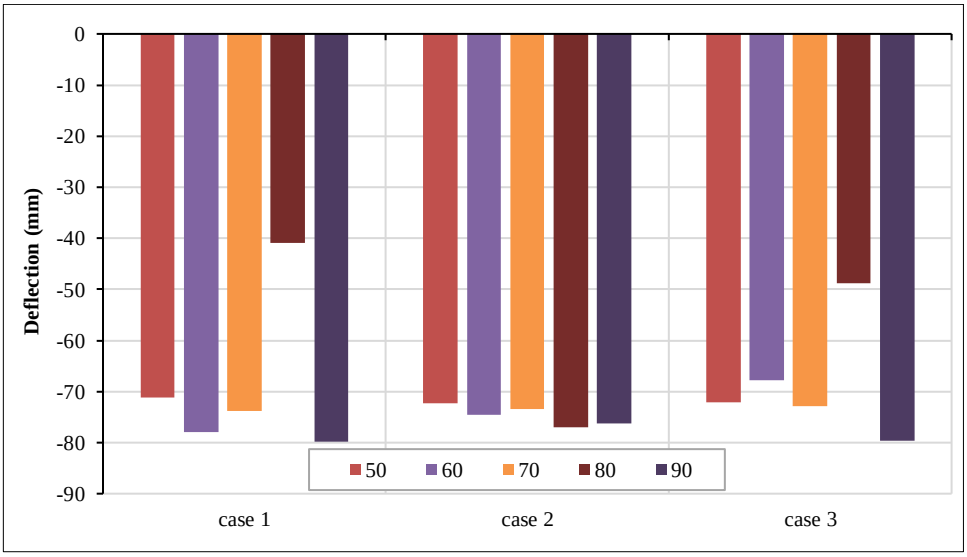

(c)

Figure 16. (a) Temperature for 500 mm of columns, (b) Time for 500 mm of columns, (c) Deflection for 500 mm of columns

Table 8. Analytical results for 500 mm of columns

Length	Type of cases	Load percentage (%)	Corresponding applied load (kN)	Temperature resisted (°C)	Time of resistance (minute)	Deflection (mm)
500 mm	Case 1	50	463.5	750.3	224.55	-71.2
		60	556.2	657.8	195.75	-78
		70	648.9	565	166.9	-73.8
		80	741.6	457.3	133.35	-40.9
		90	834.3	418	130.95	-79.8
	Case 2	50	463.5	673	226.5	-72.25
		60	556.2	322	194.13	-74.5
		70	648.9	554	166.75	-73.4
		80	741.6	491	146.8	-77
		90	834.3	444	130.28	-76.3
	Case 3	50	463.5	632	226.95	-72.1
		60	556.2	599.9	193.35	-67.88
		70	648.9	526	166.95	-72.9
		80	741.6	432	135.75	-48.9
		90	834.3	422	130.95	-79.7

5.2.3. Effect of Temperature on 750 mm of Columns

Figure 17 illustrates the effect of the temperature for a region of 750 mm of the columns. Table 9 summarizes the effect of the temperature on the columns when subjected to heating for 750 mm. Case 1 and Case 2 displayed similar trends, where there was a decrease in the capacity with an increase in the temperature, but Case 2 exhibited slightly less capacity than Case 1. Case 1 with 90% loading took less time to fail, making it critical. Case 2 with 90% loading depicted higher deflection.

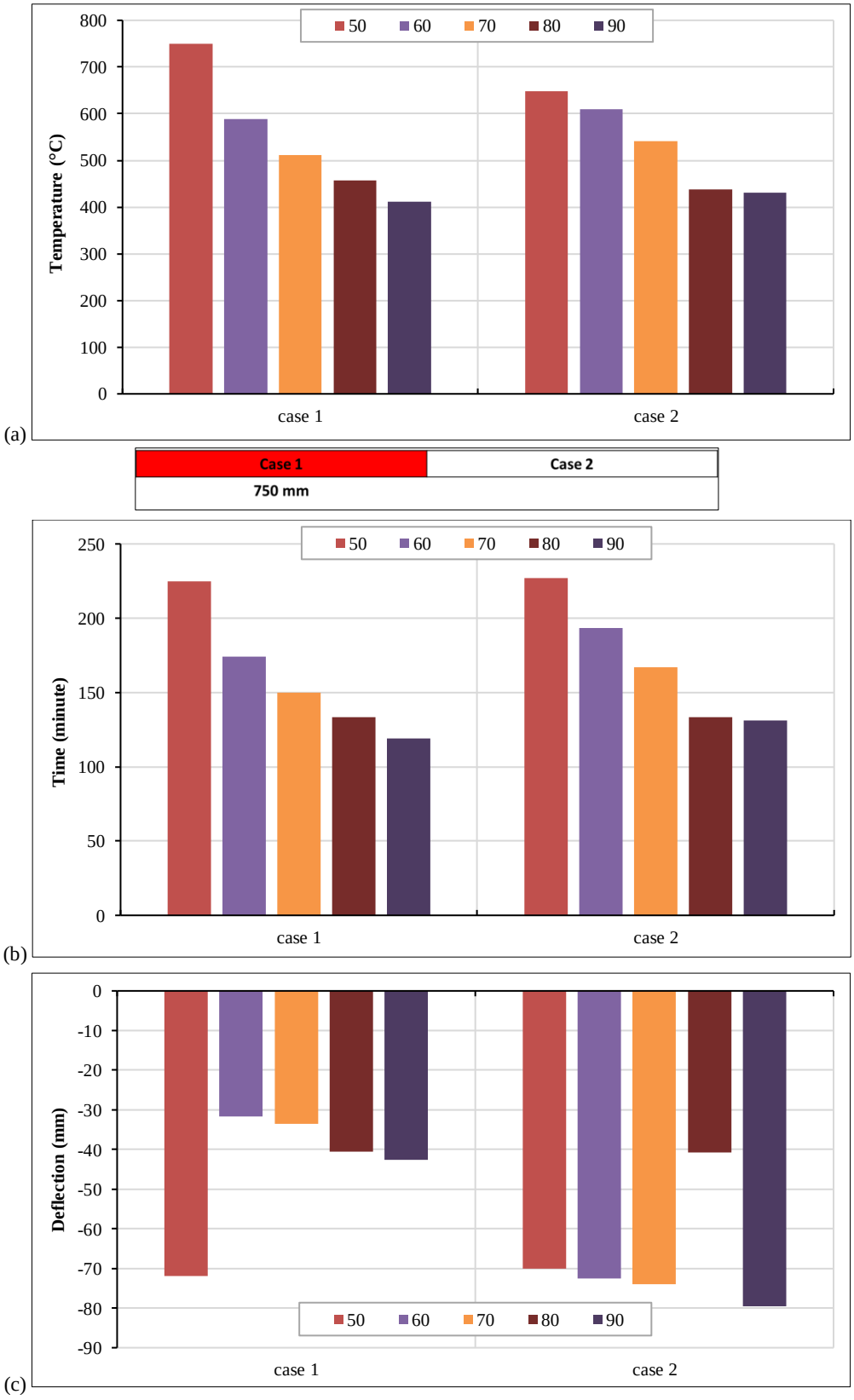

Figure 17. (a) Temperature for 750 mm of columns, (b) Time for 750 mm of columns, (c) Deflection for 750 mm of columns

Table 9. Analytical results for 750 mm of columns

Length	Type of Cases	Load percentage (%)	Corresponding applied load (kN)	Temperature resisted (°C)	Time of resistance (minute)	Deflection (mm)
750 mm	Case 1	50	463.5	750.3	224.55	-71.9
		60	556.2	588.4	174.15	-31.7
		70	648.9	511.35	150.15	-33.58
		80	741.6	457.3	133.35	-40.59
		90	834.3	411.1	118.95	-42.59
	Case 2	50	463.5	648	226.95	-70.08
		60	556.2	610.2	193.35	-72.6
		70	648.9	542	166.95	-74.06
		80	741.6	438.7	133.35	-40.7
		90	834.3	431.2	130.995	-79.6

5.2.4. Effect of Temperature on 1500 mm of Columns

The effect of the temperature for a region of 1500 mm of the columns is shown in Figure 18. Table 10 presents the effect of the temperature on the columns when subjected to heating for 1500 mm. There was a decrease in the capacity with an increase in loading, revealing faster failure when there was 90% loading compared to 50% loading. With the increase in load, there was a decrease in time for the columns to fail. The columns with 50% loading failed faster than the others. There was no uniformity in the trend, and the 60% loading case had a higher deflection than the other cases.

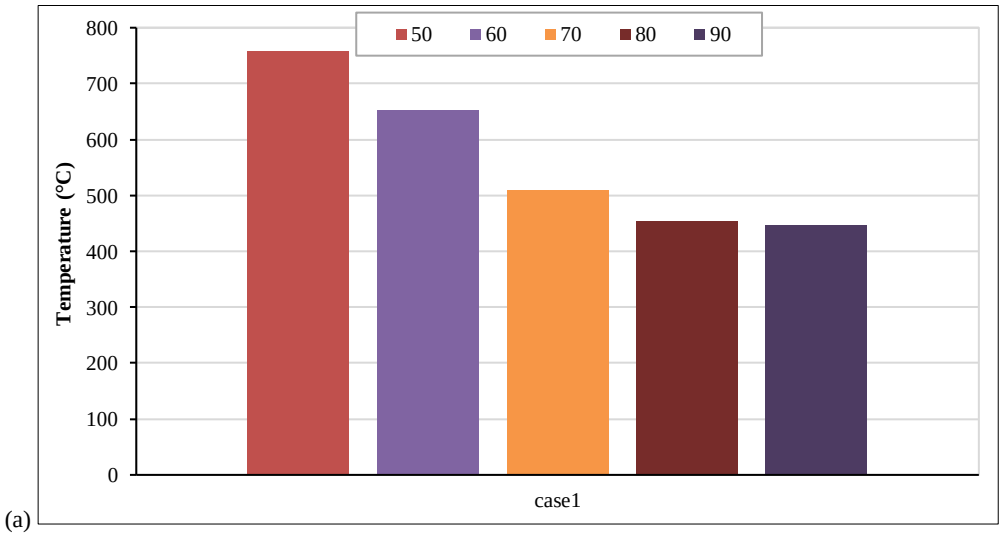

(a)

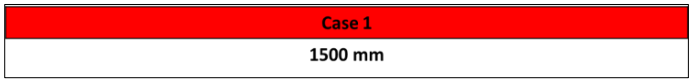

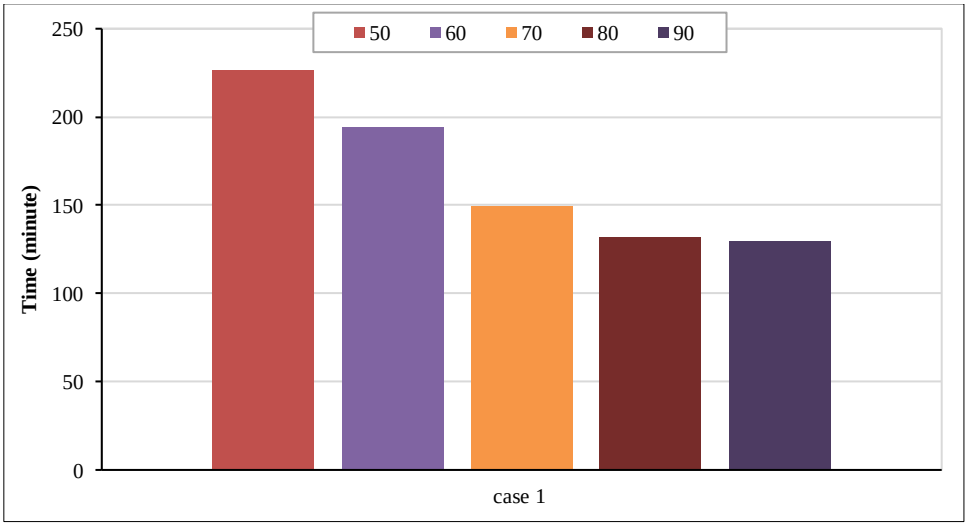

(b)

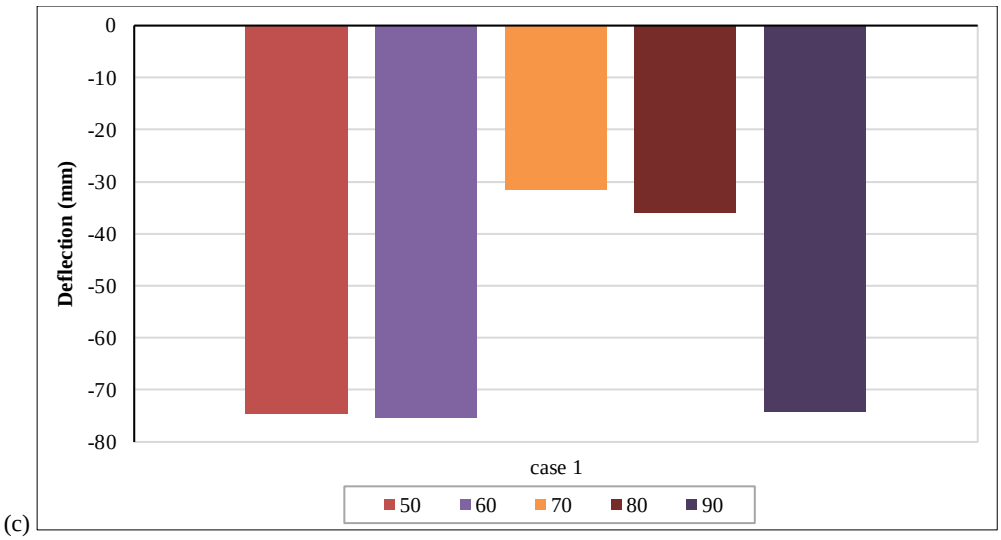

(c)

Figure 18. (a) Temperature for 1500 mm of columns, (b) Time for 1500 mm of columns, (c) Deflection for 1500 mm of columns

Table 10. Analytical results for 1500 mm of columns

Length	Type of cases	Load percentage (%)	Corresponding applied load (kN)	Temperature resisted (°C)	Time of resistance (minute)	Deflection (mm)
1500 mm	Case 1	50	463.5	757	226.6	-74.6
		60	556.2	653	194.2	-75.48
		70	648.9	509	149.4	-31.46
		80	741.6	453	131.9	-36
		90	834.3	446	129.8	-74.2

It was found that there was no uniformity in the behavior like the beams but there were several Cases where Case 1 indicated decreased strength and with the fact that the fire started from the bottom of the columns, it was critical and was taken for the Case to experiment.

6. Experimental Test Results of Beam and Column

6.1. Experimental Test Results of Beam

The beam was subjected to bending at the points of loading, and when the temperature was applied, there was a slow reduction in the deflection, illustrating the expansion of the beam, which again increased when the beam was left to unseat after 4 hours. The time versus temperature plots for various points on the beam are plotted in Figure 19, where a vertical line at 240 minutes demonstrates the heating line that separates the heating phase and cooling phase.

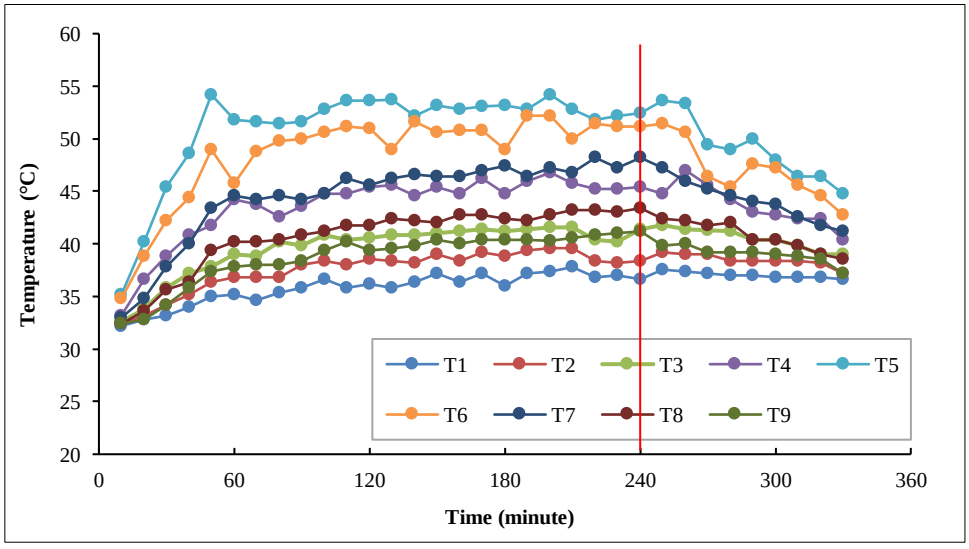

Figure 19. Temperature versus time for beam

Figure 20 provides the deflection profile at the point of loading on the left side of the beam when it was subjected to combined loading and temperature. It was found that with an increase in the temperature, the deflection decreased. The maximum deflection of 2.41 mm occurred at 10 minutes from the time of heating.

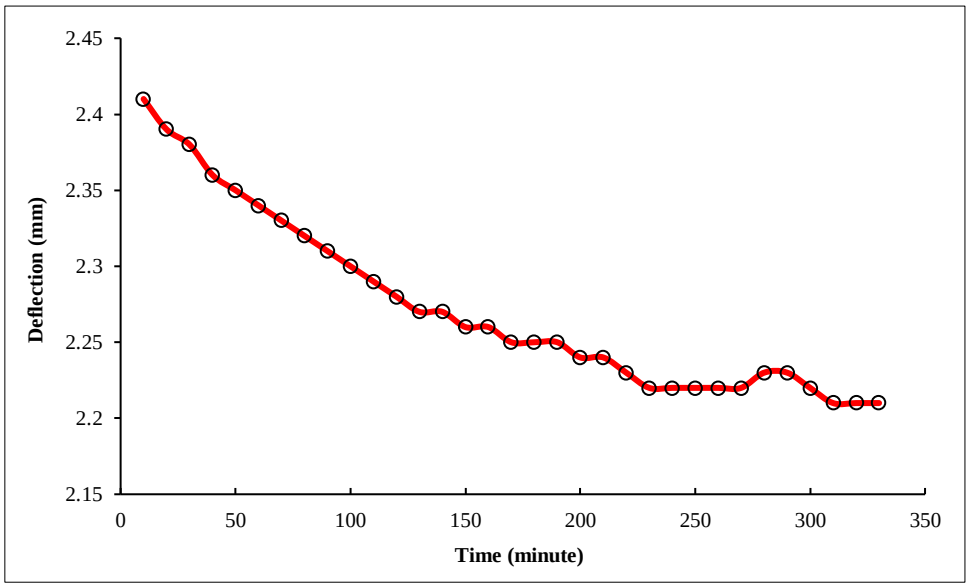

Figure 20. Deflection, left dial gauge

Figure 21 depicts the deflection profile at the point of loading on the right side of the beam when it was subjected to combined loading and temperature. The maximum deflection of 2.36 mm occurred at 10 minutes from the time of heating.

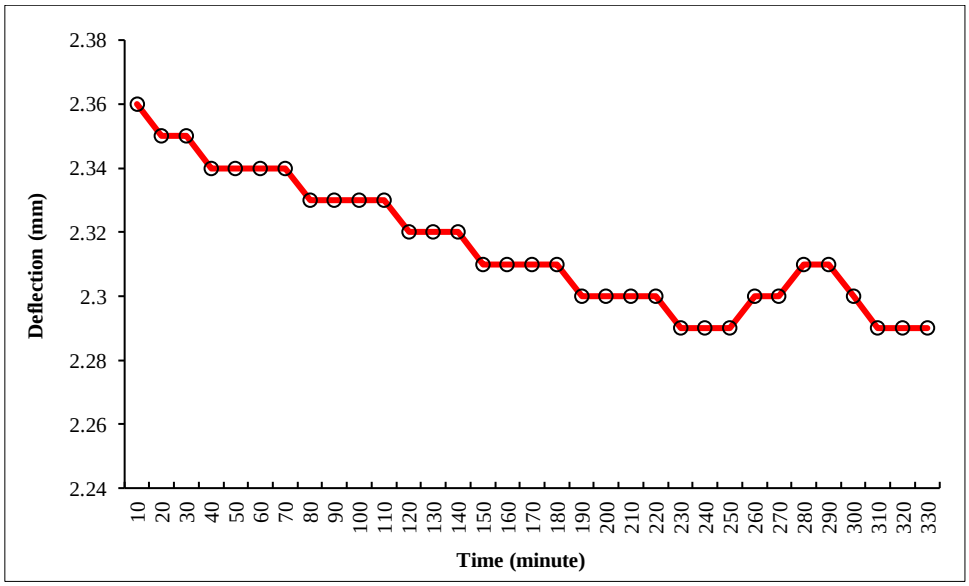

Figure 21. Deflection, right dial gauge

Deflection Check of Beam

The observed experimental and numerical deflections can be verified using the theoretical approach. From this approach, the reliability of the analysis can be verified. The deflection during loading obtained from the beam was consistent with the numerical calculations given below.

$$\text{Deflection} = \frac{Fx}{6EI}(3al - 3a^2 - x^2) = \frac{12.5\times1000\times1500}{3\times6\times2\times100000\times271.1\times10000}(3(500)(1500) - 3(500)^2 - 500^2) = 2.4 \text{ mm} \quad (1)$$

6.2. Experimental Test Results of Column

The column experienced buckling at the point where the temperature was applied, but the deflection was well within the maximum value. The buckling of the column can be seen in Figure 22. Also, Figure 23 shows the time versus temperature graph for the initial application of the temperature on the column up to 600 °C.

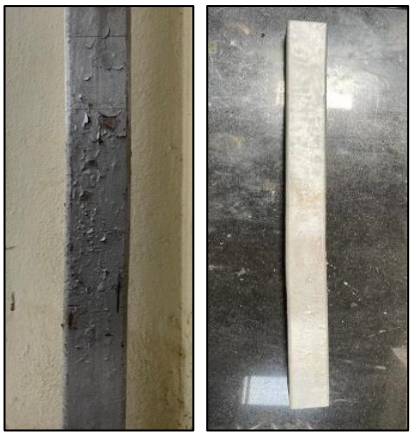

Figure 22. Buckling of column after effect of temperature

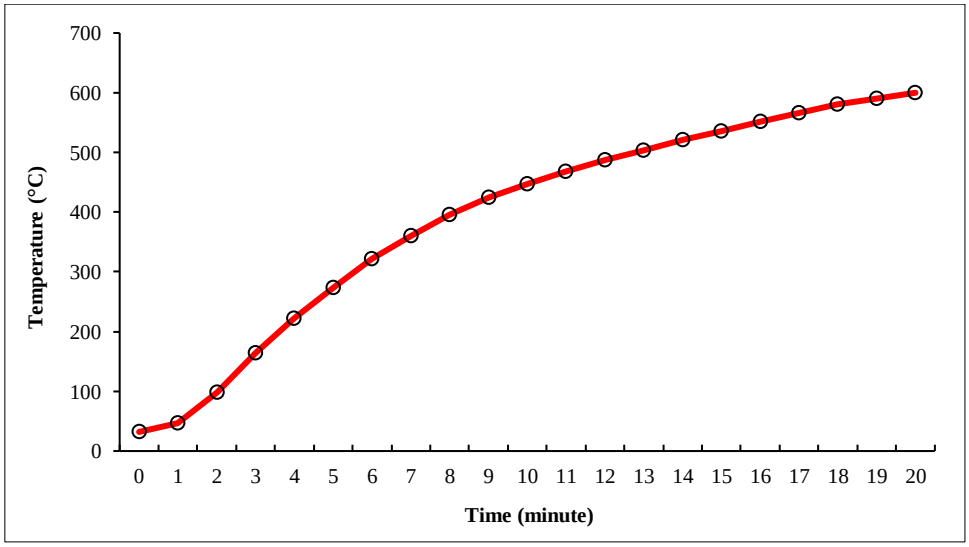

Figure 23. Initial temperature graph

There was a sudden increase in the deflection when the temperature was applied, and the deflection increased after a certain period. This was due to the expansion of steel because of the increase in the temperature. Figure 24 displays heating and cooling of the column conducted for a total of 5 hours with 4 hours of heating excluding the initial heating. There was a significant decrease in the temperature and deflection when compared to those of the beam revealing a sensitive profile even though the ability to take the temperature was higher when compared to that of the beam. Figure 25 represents the deflection profile of the column.

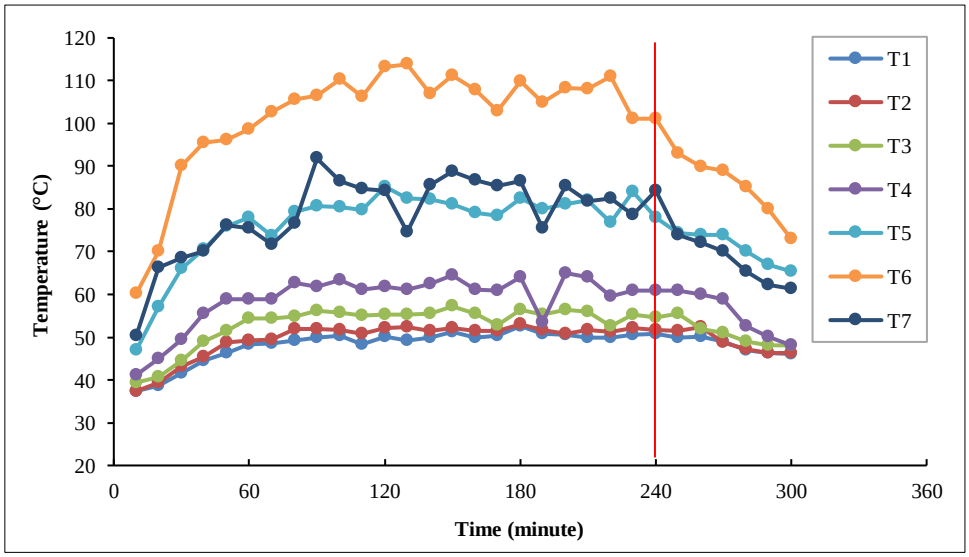

Figure 24. Temperature versus time for column

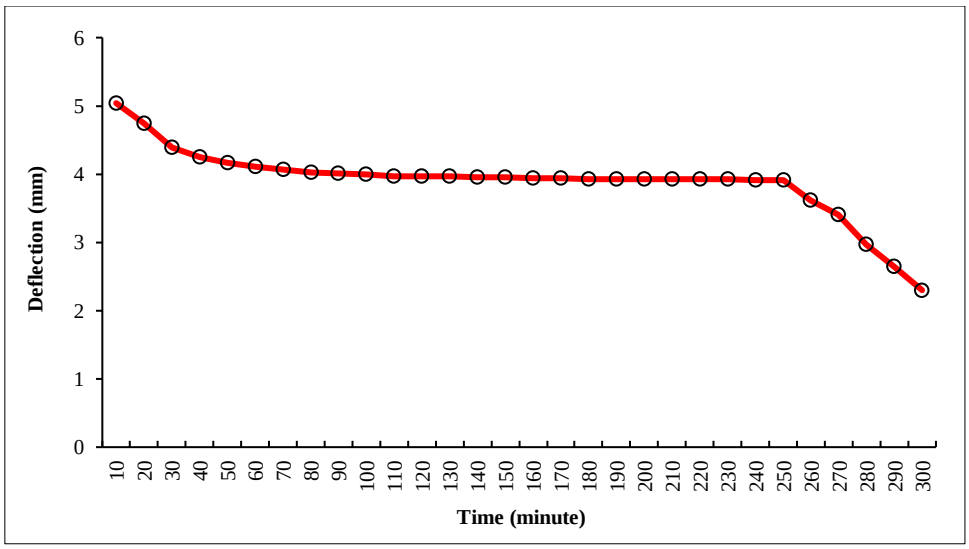

Figure 25. Deflection of column

Deflection Check of Column

The observed experimental and numerical deflections can be verified using the theoretical approach. From this approach, the reliability of the analysis can be verified. The maximum allowable deflection of the column as per IS:800-2007 [34] is:

$$\text{Deflection} = \frac{H}{150} = \frac{1500}{150} = 10 \text{ mm} \quad (2)$$

6.3. Comparison of Experimental Study and Finite Element Models

The results obtained from the experimental study of the critical beam and column were analyzed using ABAQUS, and the results of the analysis are discussed below.

6.3.1. Beam

When compared to the experimental results of the beam, the temperature in the analysis varies uniformly in time, and there are also symmetrical values on either side of the beam, which is not the case in real life. This can be observed in Figure 26, where the temperature curves of T1 and T9 overlap, which is similar in Cases T3, T4, T7, and T8. This may be due to the variation in room temperature with respect to time, the cooling effect owing to the heat loss and the capacity of the oven to maintain the temperature, and the variation in the temperature within the oven since the heat starts from the middle point of the oven and there is some difference in the heat within the oven, which is not the case in the analysis. The failure pattern of the beam is indicated in Figure 27, which is similar to that of the experimental study, which can be witnessed in Figure 28.

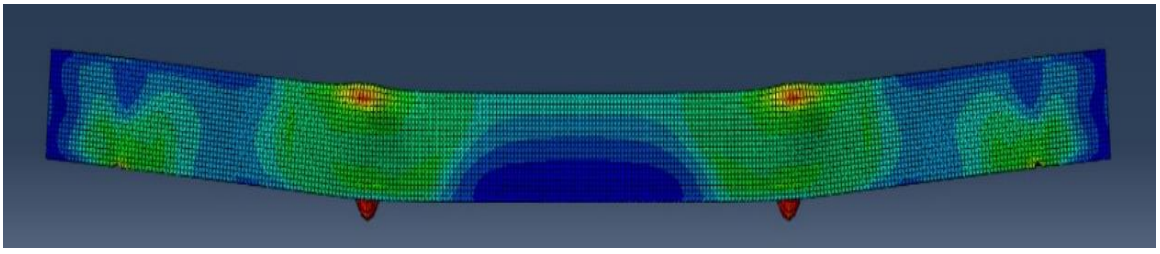

Figure 26. Failure pattern of beam in analytical study

Figure 27. Failure pattern of beam in experimental study

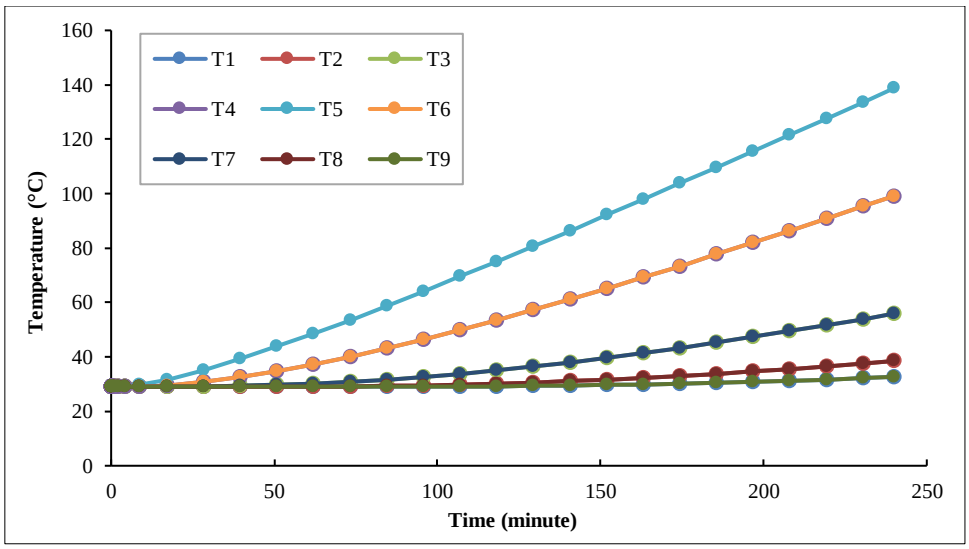

Figure 28. Temperature versus time for beam using analysis

6.3.2. Column

When compared to the experimental results of the column, the temperature in the analysis varies uniformly in time, and there are also symmetrical values on either side of the column in Cases T6 and T7, which is not the case in real life. Figure 29 illustrates the temperature variation of the points marked on the column using analysis. Figure 30 depicts the failure pattern of the column using the experimental and analytical studies.

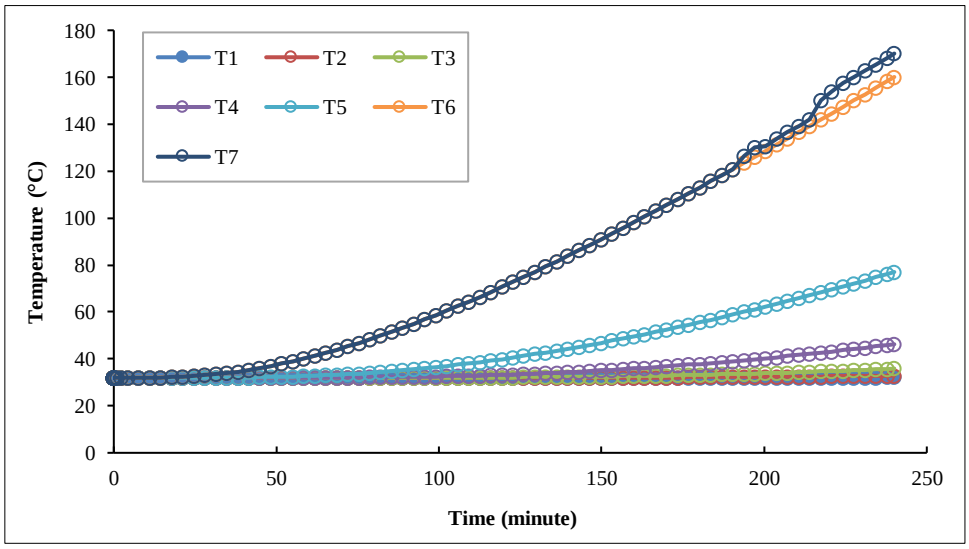

Figure 29. Temperature versus time for column using analysis

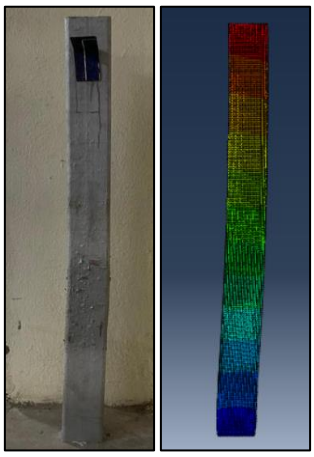

Figure 30. Failure pattern of column in experimental and analytical studies

7. Conclusions

The hollow steel section was considered for beams and columns and investigated under the elevated temperature. Different cases were considered in terms of region and load percentages. In terms of region, cases such as 250 mm, 500 mm, 750 mm, and 1500 mm were taken into account. For the load percentages, the load cases were 10%, 20%, 30%, 40%, and 50% of the ultimate load for the beams and 50%, 60%, 70%, 80%, and 90% of the ultimate load for the columns. The following conclusions were drawn from the study:

Beams

- The critical region in the beams was found to be in the middle portions, specifically in Case 3 and Case 4 for 250 mm of the beams and Case 2 for 500 mm of the beam. This may be because of the conductance of the heat on either side of the beams, which is not the case if the beams are heated from one end of the beams. Hence, it can be concluded that the middle portions of the beams are weak in terms of the elevated temperature.
- The resistance time decreased with increasing loading in all cases.
- There was a decrease in the deflection concerning the temperature and time because of the combined action of loading and expansion created due to the temperature rise, and a maximum deflection of 4.6 mm occurred in all cases with 10% loading.

Columns

- It was also found that the trend was quite similar for all the cases of the columns, where with an increase in the load, the temperature needed to reach the ultimate stress was reduced. In other words, the temperature was inversely proportional to the load. The decrease in the capacity concerning loading was 1.68 times higher in Case 1 than in the other cases; hence, it was taken to be critical.
- The resistance time also decreased with increasing loading, and there was a decrease in the resistance time of approximately 1.7 times for 90% loading when compared to 50% loading.
- There was an irregularity in the deflection concerning the temperature and time because of the combined action of loading and temperature, and a maximum deflection of 79 mm occurred when the ends of the column were subjected to the elevated temperature.
- The behavioral study of the beams and columns was conducted, and it was found that the change in the deflection concerning the temperature and time is significant for the column when compared to that of the beams based on the temperature and deflection variations obtained from the experimental study.
- The effect of the temperature on the analysis was uniform when compared to the experimental results, and the results were slightly higher compared to the experimental study.

The investigation helps the designers understand the principles while designing members to withstand fire scenarios. Furthermore, the research can be extended toward the influence of fire on beam-column sub-assemblage sections, which are meant to be more critical.

8. Declarations

8.1. Author Contributions

Conceptualization, P.M. and A.B.; methodology, P.M. and A.B.; validation, P.M., A.B., and V.M.; formal analysis, A.B. and V.M.; investigation, A.B., V.M., and A.K.; resources, A.B.; writing—original draft preparation, A.B. and A.K.; writing—review and editing, A.B. All authors have read and agreed to the published version of the manuscript.

8.2. Data Availability Statement

The data presented in this study are available in the article.

8.3. Funding

The authors received no financial support for the research, authorship, and/or publication of this article.

8.4. Conflicts of Interest

The authors declare no conflict of interest.

9. References

[1] Vishal, M., & Satyanarayanan, K. S. (2021). A review on research of fire-induced progressive collapse on structures. Journal of Structural Fire Engineering, 12(3), 410–425. doi:10.1108/JSFE-07-2020-0023.

[2] Zhong, Y., Su, A., & Zhao, O. (2023). Post-fire local buckling behaviour of cold-formed S700 high strength steel circular hollow sections under axial compression: Experiments, modelling and design. Thin-Walled Structures, 184, 110511. doi:10.1016/j.tws.2022.110511.

[3] Khoury, G. A. (2000). Effect of fire on concrete and concrete structures. Progress in Structural Engineering and Materials, 2(4), 429–447. doi:10.1002/pse.51.

[4] Vishal, M., & Satyanarayanan, K. S. (2022). Experimental investigation on the heat dissipation and postfire structural performance of a reinforced concrete column with biomimicked geometry. Fire, 5(6), 205. doi:10.3390/fire5060205.

[5] Huang, B., Qiu, X., Zhu, J., Song, H., & Zhang, Z. (2023). Residual performance of compression stiffened welded hollow spherical joints after exposure to elevated temperatures. Journal of Constructional Steel Research, 208, 108001. doi:10.1016/j.jcsr.2023.108001.

[6] Agha, A., Shibani, A., Hassan, D., & Zalans, B. (2021). Modular construction in the United Kingdom housing sector: barriers and implications. Journal of Architectural Engineering Technology, 10(2), 236.

[7] Vishal, M., & Satyanarayanan, K. S. (2023). Study on optimum concrete cover thickness in RC beam and columns under high temperature. Journal of Structural Fire Engineering, 14(4), 461–480. doi:10.1108/JSFE-11-2022-0035.

[8] Ferdous, W., Bai, Y., Ngo, T. D., Manalo, A., & Mendis, P. (2019). New advancements, challenges and opportunities of multi-storey modular buildings – A state-of-the-art review. Engineering Structures, 183, 883–893. doi:10.1016/j.engstruct.2019.01.061.

[9] Cao, X., Li, X., Zhu, Y., & Zhang, Z. (2015). A comparative study of environmental performance between prefabricated and traditional residential buildings in China. Journal of Cleaner Production, 109, 131–143. doi:10.1016/j.jclepro.2015.04.120.

[10] Weerasinghe, P., Samarasinghe, T., Gunawardena, T., Nguyen, K., Mendis, P., Ngo, T., & Aye, L. (2018). An optimum construction strategy for multi-story residential prefabricated modular buildings. ZEMCH 2018 International Conference, 29-1 January, 2018, Melbourne, Australia.

[11] Boafo, F. E., Kim, J. H., & Kim, J. T. (2016). Performance of modular prefabricated architecture: Case study-based review and future pathways. Sustainability, 8(6), 558. doi:10.3390/su8060558.

[12] Bertram, N., Fuchs, S., Mischke, J., Palter, R., Strube, G., & Woetzel, J. (2019). Modular construction: From projects to products. McKinsey & Company, New York, United States.

[13] Kalam, L. (2021). Finite Element Analysis of Complex Vectorbloc Beam-Column Connections. Ph.D. Thesis, University of Windsor, Windsor, Canada.

[14] Lee, J., & Kim, J. (2017). BIM-Based 4d simulation to improve module manufacturing productivity for sustainable building projects. Sustainability (Switzerland), 9(3), 426. doi:10.3390/su9030426.

[15] Kamali, M., & Hewage, K. (2016). Life cycle performance of modular buildings: A critical review. Renewable and Sustainable Energy Reviews, 62, 1171–1183. doi:10.1016/j.rser.2016.05.031.

[16] Wu, C., Zhou, Y., Liu, J., Mou, B., & Shi, J. (2021). Experimental and finite element analysis of modular prefabricated composite beam-column interior joints. Journal of Building Engineering, 43(May), 102853. doi:10.1016/j.jobe.2021.102853.

[17] Kumar, W., Sharma, U. K., & Pathak, P. (2023). Comparison of mechanical and structural performance of fire-resistant steels at elevated temperatures. Structures, 48, 478–491. doi:10.1016/j.istruc.2022.12.103.

[18] Kim, S., Hong, W. K., Kim, J. H., & Kim, J. T. (2013). The development of modularized construction of enhanced precast composite structural systems (Smart Green frame) and its embedded energy efficiency. Energy and Buildings, 66, 16–21. doi:10.1016/j.enbuild.2013.07.023.

[19] Nahmens, I., & Ikuma, L. H. (2012). Effects of lean construction on sustainability of modular homebuilding. Journal of architectural engineering, 18(2), 155–163. doi:10.1061/(asce)ae.1943-5568.0000054.

[20] Ramaji, I. J., & Memari, A. M. (2013). Identification of structural issues in design and construction of multi-story modular buildings. Proceedings of the 1st residential building design and construction conference, 20-21 February, 2013, Bethlehem, United States.

[21] Harrison, B. F. (2003). Blast resistant modular buildings for the petroleum and chemical processing industries. In Journal of Hazardous Materials, 104(1–3), 31–38. doi:10.1016/S0304-3894(03)00232-2.

[22] CCHPR (2023). CCHPR Launches New Report on Modular Homes. Department of Land Economy, University of Cambridge, Cambridge, United Kingdom. Available online: https://www.landecon.cam.ac.uk/news/cchpr-launches-new-report-modular-homes (accessed in October 2023).

[23] Yu, Y., Tian, P., Man, M., Chen, Z., Jiang, L., & Wei, B. (2021). Experimental and numerical studies on the fire-resistance behaviors of critical walls and columns in modular steel buildings. Journal of Building Engineering, 44(July), 102964. doi:10.1016/j.jobe.2021.102964.

[24] Arrais, F., Lopes, N., & Vila Real, P. (2023). Fire design of stainless steel columns with hollow circular and elliptical sections. Journal of Constructional Steel Research, 210, 108085. doi:10.1016/j.jcsr.2023.108085.

[25] Chen, Z., Liu, J., & Yu, Y. (2017). Experimental study on interior connections in modular steel buildings. Engineering Structures, 147, 625–638. doi:10.1016/j.engstruct.2017.06.002.

[26] Gardner, L., Saari, N., & Wang, F. (2010). Comparative experimental study of hot-rolled and cold-formed rectangular hollow sections. Thin-Walled Structures, 48(7), 495–507. doi:10.1016/j.tws.2010.02.003.

[27] Mohammed, A., & Afshan, S. (2023). Modelling and design of stainless steel hollow section beam-column members in fire. International Journal of Steel Structures, 23(1), 120–138. doi:10.1007/s13296-022-00683-2.

[28] Yan, J. B., Cao, J., Xie, P., Li, N., & Xie, J. (2023). Circular hollow stainless-steel tubes subjected to low-temperature eccentric compression loads. Structures, 54, 1164–1178. doi:10.1016/j.istruc.2023.05.092.

[29] Gatheeshgar, P., Poologanathan, K., Gunalan, S., Shyha, I., Sherlock, P., Rajanayagam, H., & Nagaratnam, B. (2021). Development of affordable steel-framed modular buildings for emergency situations (Covid-19). Structures, 31(2121), 862–875. doi:10.1016/j.istruc.2021.02.004.

[30] AISI S100-16. (2016). North American Specification Steel Structural Members. American Iron and Steel Institute, Washington, United States.

[31] EN 1991-1-7. (2006). Eurocode 1: Action on structures - Part 1-7: General actions - Accidental actions. European Committee for standardization, Brussels, Belgium.

[32] Kesawan, S., & Mahendran, M. (2018). Post-fire mechanical properties of cold-formed steel hollow sections. Construction and Building Materials, 161, 26–36. doi:10.1016/j.conbuildmat.2017.11.077.

[33] Luo, F. J., Ding, C., Styles, A., & Bai, Y. (2019). End plate–stiffener connection for SHS column and RHS beam in steel-framed building modules. International Journal of Steel Structures, 19(4), 1353–1365. doi:10.1007/s13296-019-00214-6.

[34] IS:800-2007. (2007). Indian Standard Code of Practice for General Construction in Steel. Bureau of Indian Standards, New Delhi, India.